ISSN 2314-5609
Nuclear Sciences Scientific Journal
12, 1-23
2023
https://nssi.journals.ekb.eg

PETROGENESIS AND TECTONIC EVOLUTION OF THE RING COMPLEXES IN SOUTH EASTERN DESERT, EGYPT: A CASE STUDY FROM EL-GEZIRA ALKALINE ASSOCIATION

ABDELHADY RADWAN; ASHRAF EMAM; GEHAN B. ELSHAYEB[1] and MOHAMMED H. YOUNIS

Geol. Dept., Aswan Fac. Sci., Aswan Univ., Aswan 81528, Egypt ; Nuclear Materials Authority, Cairo, Egypt[1]

ABSTRACT

El-Gezira ring complex represents an important alkaline association in the south Eastern Desert, Egypt display crescent-shaped bodies and vast diversity of lithologies. It consists of several concentric rings separated by arch-shaped bodies of alkali gabbros, pyroclastics and hybrid rocks. The outer ring of El Gezira is composed of metavolcanics and basaltic andesitic flows. The inner part comprises carbonate, pyroxene bearing syenite, monzosyenite, trachyte, trachy-andesite and trachydacite. Clinopyroxenes are the prevailing mafics components in most rocks varieties. Amphiboles and olivine are common in most basic units. El Gezira ring complex comprises a high fractures frequency. El Gezira ring complex is one of a major cluster of ring complexes aligned along an ENE transform fault in the extreme southern part of Egypt. Chemically, El Gezira rock- associations are mostly metaluminous, and show low concentrations of CaO, MgO and Sr. Moreover alkalis, Rb, Nb, Y, and REE are relatively high which is distinctive of anorogenic affinity. The alkali gabbros have flat REE patterns with slight positive Eu anomalies. The trachyandesite, trachydacite and monzosyenite all have weakly to moderately fractionated patterns with a general enrichment in LREE, and mostly possess a pronounced positive and negative Eu anomalies. Typically, El-Gezira alkaline associations are classified as within plate granites. It is suggested that the primitive mantle mafic magmas were emplaced into intracrustal magma chambers during extensional regime. The primitive magma underwent fractionation processes to give the highly evolved liquids. Influx of more hot primitive magma may promote dynamic convection, crustal assimilation and eruption of the volcanic alkaline association filling fractures during post orogenic regimes.

INTRODUCTION

A ring complex is a general term used to describe an intrusive complex that contains cone sheets and/or ring dikes. Complexes containing only cone sheets or ring dikes are occasionally called cone-sheet complexes and ring-dike complexes, respectively. Ring complexes have long been thought to represent transitional links between calderas and their underlying magma chambers (Williams 1941; Richey 1948; Turner 1963; Smith and Bailey 1968, and Oftedahl 1978). In the North East African province, more than 130 ring complexes have been emplaced during Pan Afri-

can times and continued through one or more successive periods of Phanerozoic magmatism (Black et al. 1985; and Vail 1985, 1989). In the Egyptian Nubian Shield, the alkaline associations are mostly concentrated at the South Eastern Desert (Fig. 1). Most assembly of these structures are generally aligned around the central African parallel trends. These lineaments cut across the African plate from Cameroon in the west to the Red Sea Hills of Sudan (Schandelmeier and Pudlo 1990). The ring complexes of Egyptian Shield paid attention of many studies due to the opportunity of their enrichment by many rare metal mineralizations (El Ramly et al. 1970; El Ramly and Hussein 1985). Garson and Krs (1976)

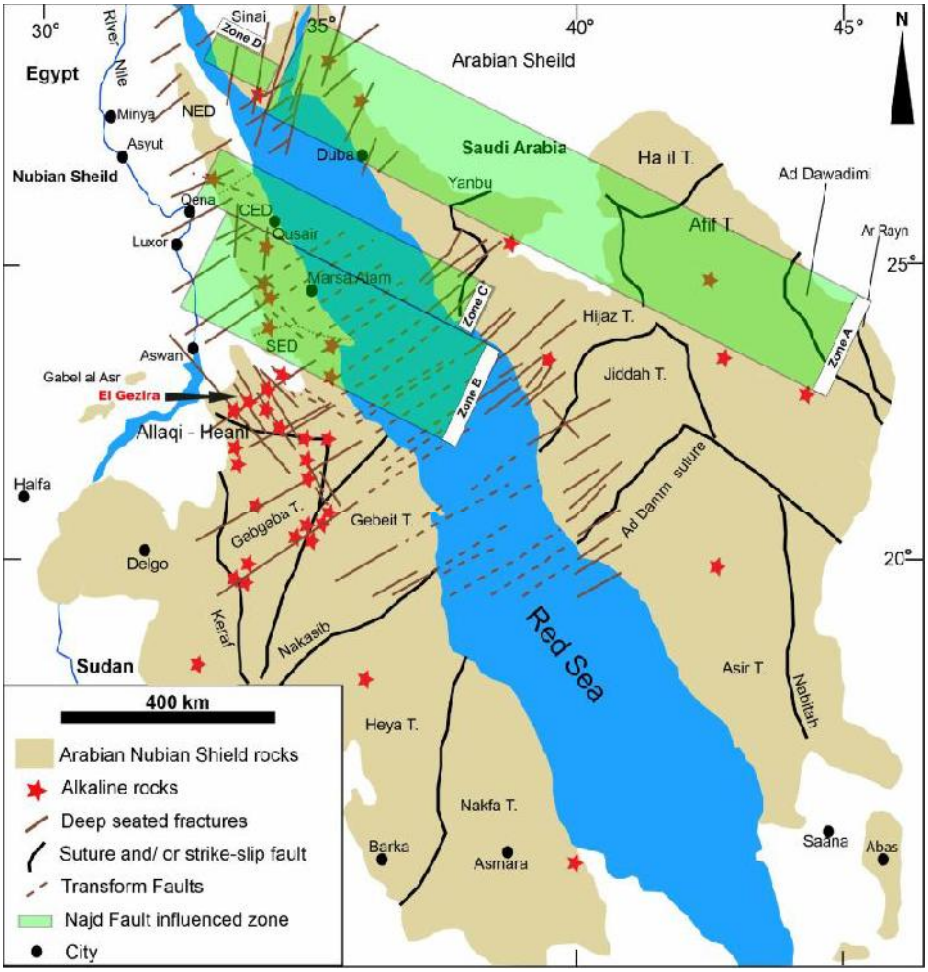

Fig. 1: Geologic map of the Arabian–Nubian Shield shows the locations of alkaline intrusions (modified from Johnson et al., 2011), distributions of deep seated tectonic lineaments after Garson and Krs (1976), zones influenced by the Najd Fault System and the related major shear zones (after Fowler and Hamimi, 2020). Najd zone based on (a) Arabian shield faults system and (b) NED transform model, (c) extension of Najd into the Sinai, (d) Najd fault zone between the Duwi fault (DFZ) zone and Wadi Kharit- Wadi Hodein shear zone (KHSZ)

concluded that the N60°E fault corridor is the main controlling structure for allocation of the post orogenic ring structures in SED. El Ramly et al., 1971; El Ramly and Hussein, (1985) have ascribed the alkaline rocks of SED to some uniformity along lines of weakness (zones of rift) probably during Precambrian age which enjoyed rejuvenation at later times. In Egypt, the ring complexes are exemplified as circular dykes, blocks and volcanic influxes invading the upper Proterozoic Pan-African basement associations (El Ramly et al. 1971; El Gaby et al. 1988). The ring complexes of Egypt include a wide spectrum of rock types that are mainly alkaline to peralkaline granites and syenites, with subordinate trachyte, rhyolite, nephelene syenite, agglomerate and occasional presence of some basaltic trachy-andesite and carbonates (Hashad and El Reedy 1979; El Ramly and Hussein 1982, 1985).

The present study attempts to address the main petrological, geochemical and structural features of the alkaline association forming El Gezira ring complex. The main objective of this study is to discuss and evaluate the magmatic history, petrogenesis and geodynamic setting of El Gezira ring complex in response to the deformation history of SED.

METHODOLOGY

For the whole rock chemistry of El-Gezira ring complex, 15 representative samples were chemically analyzed for major, trace and rare earth elements as three samples for each rock type. The analyses were accomplished at (ACME) Labs, Canada. The total abundances of major and minor oxides were elucidated through using inductively coupled plasma (ICP)-emission spectrometry, while the trace and rare earth elements were determined by using the ICP-mass spectrometry. U and Th elements were detected using the ICP-emission spectrometry.

GEOLOGICAL SETTING

El-Gezira ring complex is located at the extreme South Eastern Desert at the intersection of two conjugate main wadies: Wadi Um Gir and Wadi Naqit. It lies between lat. 22° 16' 00 and 22° 18' 30' N, and long. 33° 39' 00 and 33° 42' 00 E. It has crescent-shaped outline and is slightly elongated in the northeastern direction with 3.5 km width and elevation of 483 m (Fig. 2a). El-Gezira alkaline associations are emplaced through suite of Precambrian igneous and metamorphic associations of Proterozoic age (Fig. 2b). The rocks form El Gezira exhibit a high degree of differentiation and represented by a wide spectrum of lithologies. The complex is formed from central mass, inner and outer rings, separated by two wadis. The metavolcanics surrounded the outer ring and is composed essentially of basaltic flows, tuffs and agglomerates. These basaltic arcs are followed inward with arch shaped blocks and lenses of alkali gabbros especially in the southern part of the ring separating between the outer and inner rings. The inner ring is incomplete and composed of carbonate, pyroxene bearing syenite, monzosyenite, trachyte, trachy-andesite and trachydacite. On the other hand, the central mass is more complicated forming conspicuous ridges and formed essentially of alkaline syenite (Figs. 2a & 2b). In the north eastern part of the central mass, a stock-like body of coarse grained syenite with relics of trachyandesite and trachydacite are observed. El Gezira alkaline association is dissected by two wrench fault systems with NE-SW and NW-SE directions.

PETROGRAPHIC FEATURES

Alkali Gabbro (essexite)

Essexite gabbro constitutes the outer part of the complex. It consists of plagioclase, olivine, amphiboles and rare clinopyroxene. Nepheline, biotite and microcline occur as subordinate (Figs. 3,4,5). Apatite, zircon opaque oxides and are the main accessories (Fig.3). Most plagioclase are zoned, augite grains are mostly completely replaced by amphiboles (Figs. 4,5). Some olivine crystals are replaced by chlorite streaks. Biotite shows

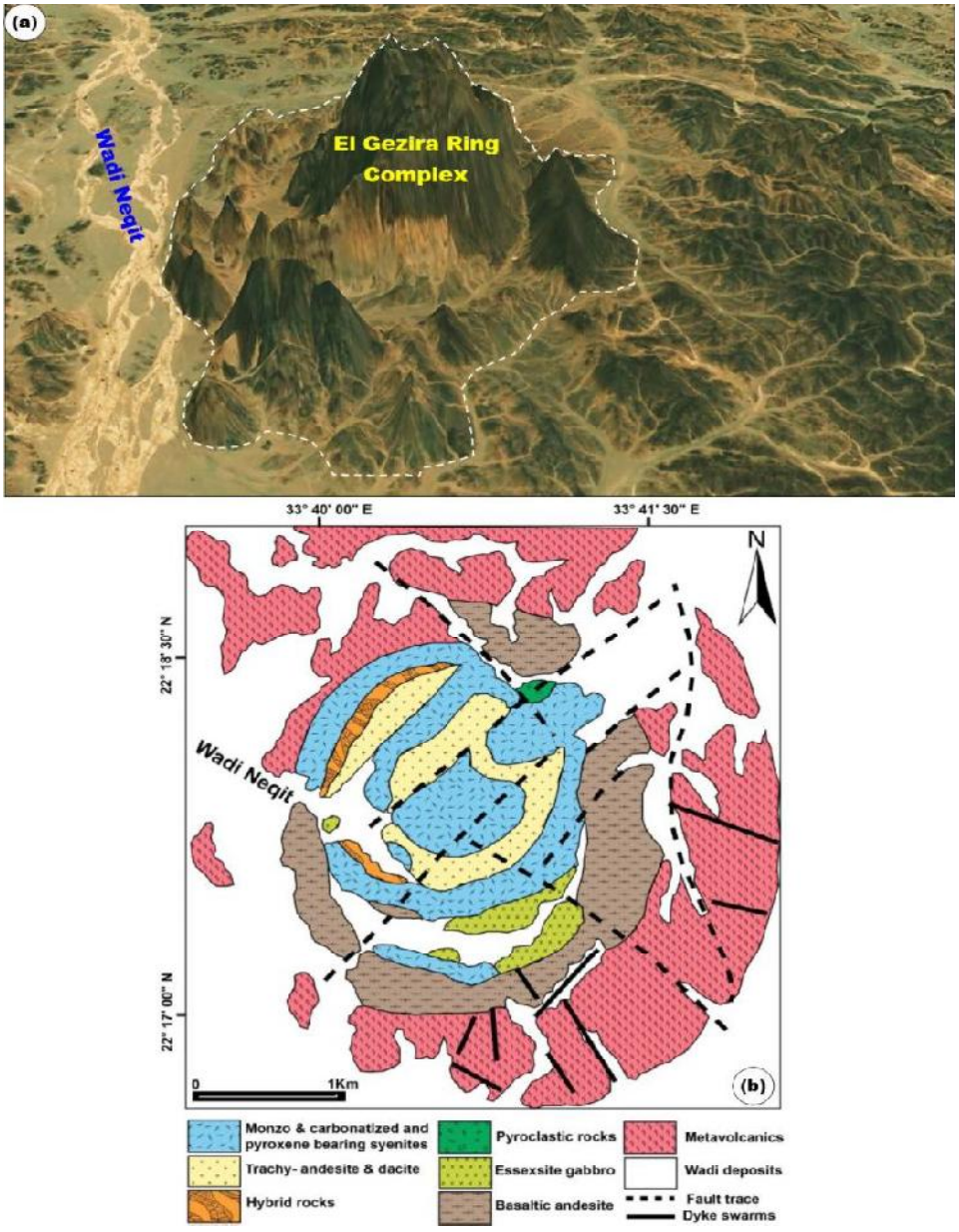

Fig. 2 : a) Arc-gis earth 3D image showing the high relief and the circular outcrop of El-Gezira ring complex, b) Geological map of El-Gezira alkaline association modified from Mohamed (1998)

irregular phenocrysts and enclosed opaque minerals along their cleavage planes. Most microcline grains are altered and enclosed zircon and sericite minute crystals along their surfaces (Figs.3,4). Dissolved textures are widely observed in which, pyroxene is altered to amphibole (Fig. 3b), and biotite is transformed to fibrous chlorites (Fig.4).

Basaltic Andesite

Basaltic andesite consisting of plagioclase, pyroxene, amphibole, and biotite. Sericite, epidote and calcite are the main accessories. Apatite and opaques are the main accessories. Plagioclase has large subhedral and unhedral phenochrysts. Subhedral crystals are generally largely sericitized and Saussuritized which obliterate the common twining. anhedral plagioclase show partially resorbed embayed shapes that generally filled with small brownish veinlets (Figs.6,7). Quartz has fine grains aggregates scattered in the groundmass. The coarser crystals may exhibit interlocking shapes that filled interstitial spaces in the matrix. The pyroxene and amphiboles have small subhedral grains scattered in the groundmass mostly have bright birefringence.

Trachytic Rocks

Trachyte : It is bright rock, that consist of orthoclase and quartz laths within brownish

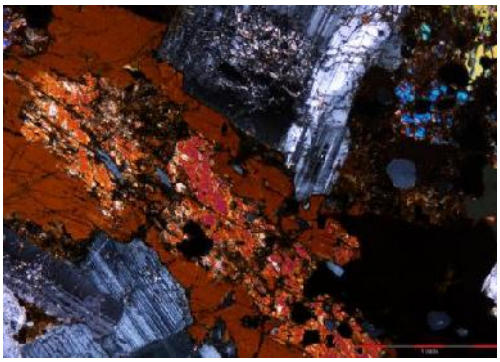

Fig.4: Microscopic photo showing uralitization processes of alkali gabbro

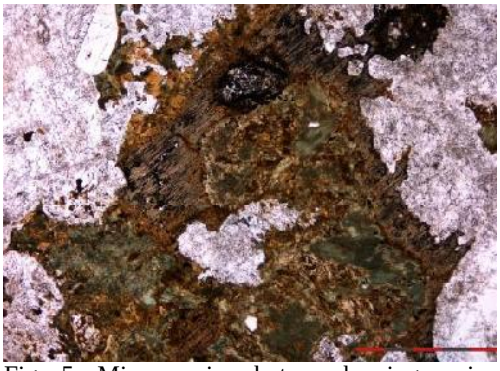

Fig. 5. Microscopic photo showing major components and dissolution textures in essexite

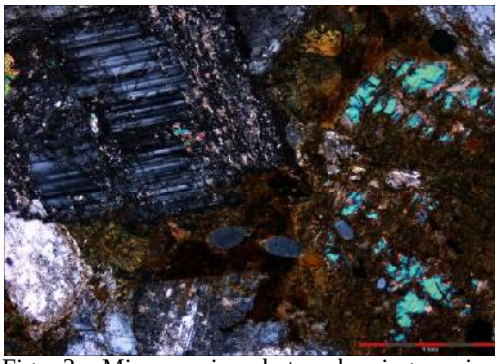

Fig. 3. Microscopic photo showing major constituents of essexite gabbro

Fig.6: Microscopic photo showing resorbed phenocryst of feldspar in basaltic andesite.

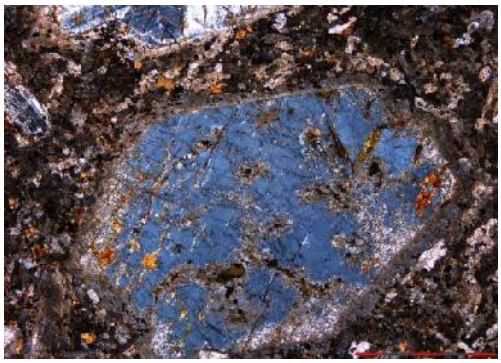

Fig.7 : Microscopic photo showing euhedral plagioclase filled with veinlets and corroded by other components within groundmass forming the porphyritic texture in basaltic andesite

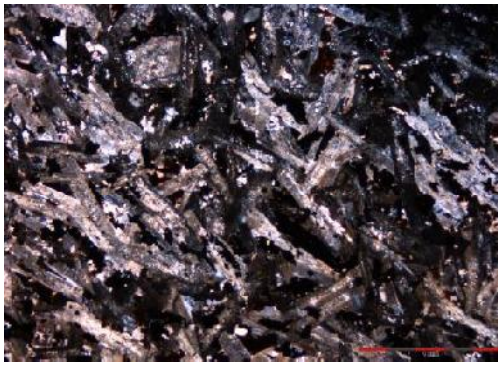

Fig. 8: Microscopic photo showing parallel alignments of quartz and feldspars forming directive texture in trachyte

groundmass. The alkali feldspar megacrystals have resorbed margins and overgrown by quartz and other constituents of the groundmass forming directive texture which is characteristic of trachyte (Fig. 8). Mafic minerals phases occur as minute dark green aggregates scattered in the matrix. Large alkali-feldspars phenocrysts mostly carbonatized and may be sericitized. Opaque oxides occur as dark and brownish spots with random distributed in the matrix.

Trachy-andesite : It is dark green and grey colors. It consists of plagioclase, pyroxene and alkalifeldspars in fine grained groundmass of feldspars, amphiboles and biotite. Apatite and iron oxides are main accessories. Most plagioclase phenocrysts are zoned. Fine flakes and aggregates of reddish biotite are mostly overgrown upon both amphibole and pyroxene cleavages. Apatite occurs as lobate inclusions in pyroxene or scattered in the matrix. Iron oxides are the dominant oxide with random distribution in the groundmass.

Trachy-dacite : It is highly a leucocratic rock that consists of alkali feldspar large laths in a fine grain albite. The alkali feldspar phenocryst has resorbed margins, and is overgrown by the minerals from the matrix (Fig.9). Quartz exists as fine and pulverized aggregates in the groundmass. Mafic phase

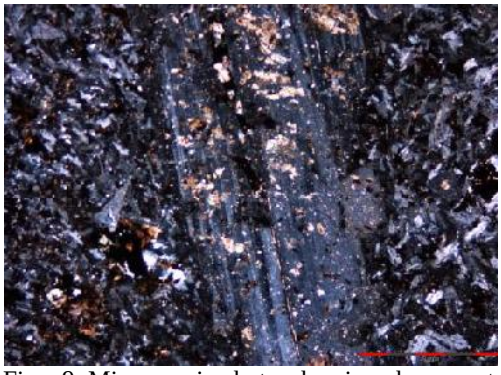

Fig. . 9: Microscopic photo showing phenocryst of carbonatized plagioclase, quartz, alkali-feldspars and cryptocrystalline mafics in trachydacite

are cryptocrystalline and occur as dark green minute grains in the matrix. Opaques occur as mafic clusters that have random distribution in the matrix.

Syenite

It includes (monzosyenite, aegirine bearing syenite and carbonatized syenite):

The monzosyenites : These are medium- to coarse-grained rocks consist of aegirine, hornblende, nepheline, microcline and biotite, with opaques and apatite as accessories (Fig.10). Aegirine occurs as subhedral to eu-

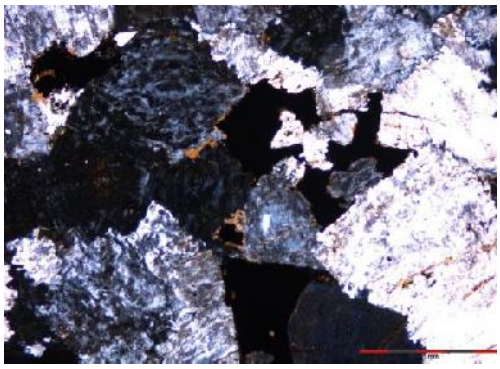

Fig. 10: Microscopic photo showing perthite, biotite, and equigranular texture of monzosyenite

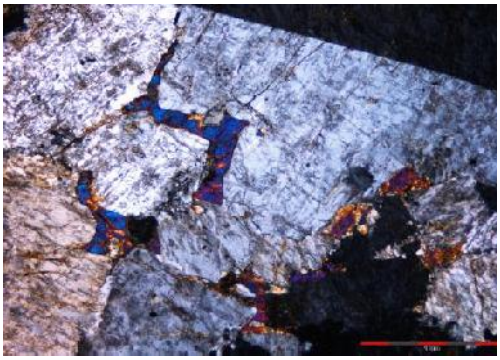

Fig. 11: Microscopic photo showing aegirine crystals filling interspaces in syenite

hedral grains with high interference colors. It forms ragged and shreds enclosed within feldspars crystals. Elongate biotite flakes commonly corrode and overgrowths upon amphiboles and pyroxenes that lead to the liberation of opaque clots apatite is common as euhedral lobate inclusions within mafic phases.

Aegirine bearing syenite : It has a higher modal proportion of pyroxene, biotite and opaques compare with monzosyenite (Fig.11). Muscovite occurs as small aggregates scattered in the groundmass. Biotite may replace pyroxene lead to the formation of chlorite and opaque oxides as products. Sometime syenite is highly carbonatized showing wide frequency of carbonates that are mainly calcite, and dolomite. They show high birefringence and filling the interspaces between other constituents in the groundmass (Fig.12).

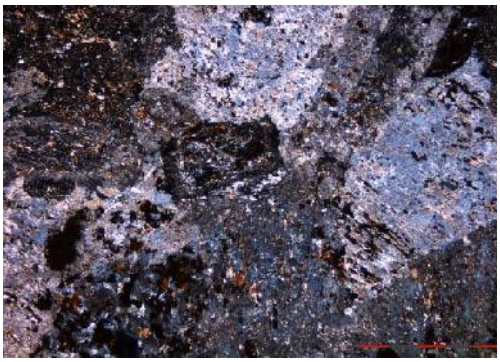

Fig. 12: Microscopic photo showing highly carbonatized alkali feldspars in syenite

WHOLE ROCK CHEMICAL CHARACTERISTICS

The results of geochemical data of El-Gezira alkaline rocks are given in (Table 1). The studied association shows a narrow range of silica average (57.88 wt %) and high abundances of total alkalis (3.76–12.7 wt %), Al_2O_3 (12.3–17.78 wt %) and CaO (0.63–8.87 wt %). The association also shows high FeO_t and low TiO_2 with averages as 8.72 and 1.00, respectively. The rocks of El-Gezira ring complex have been classified using Winchester and Floyd (1977) diagram (Fig. 13) on which they fall in the trachyte, trachyandesite, sub-alkaline- basalt, and phonolite. According to Le Bas et al. (1986) diagram, the rocks lie in trachyte, trachydacite, trachyandesite, trachybasalt and basalt fields (Fig. 14). Moreover, all rocks are characterized by high FeO_t/ (FeO_t + MgO) ratios (0.59 – 0.99) and show a ferroan nature on Frost et al. (2008) diagram (Fig.15). The high alumina index (AI = 0.96–1.52, Table 1) of the studied association clearly reflects their alkaline signature (Liégeois et al. 1998). This alkaline affinity is further supported by

Table 1: Major oxides, selected trace elements, fractionation indexes and CIPW norm of alkaline rocks from El-Gezira area

Rock type	Alkali gabbro			Basaltic andesite			Trachyte			Syenite			Trachydacite		
Sample No.	3	11	14	8	13	18	15	19	20	6	10	12	17	25	2
SiO_2	50.62	51.70	49.88	55.81	54.97	55.37	58.69	59.30	57.94	61.44	59.89	59.11	67.04	64.10	62.32
TiO_2	2.22	0.73	1.36	1.29	1.36	2.38	0.68	0.98	1.31	0.47	0.69	0.75	0.17	0.24	0.42
Al_2O_3	17.17	16.72	16.55	17.78	16.74	16.53	15.94	15.97	15.62	16.33	17.17	16.00	12.30	16.49	16.17
FeOt	11.60	9.33	10.47	8.77	8.94	9.78	9.32	8.95	9.17	7.83	7.48	8.92	7.72	5.53	6.96
MnO	0.24	0.14	0.11	0.19	0.17	0.21	0.20	0.17	0.24	0.16	0.14	0.19	0.10	0.11	0.14
MgO	2.42	8.33	6.48	1.14	2.65	1.43	0.36	0.86	0.87	0.57	0.33	0.40	0.23	0.22	0.07
CaO	7.22	8.87	8.83	4.46	5.57	5.21	3.67	2.78	3.34	2.80	3.78	2.43	1.27	0.63	0.31
Na_2O	4.82	2.35	3.74	6.85	4.62	4.77	7.04	6.57	6.12	5.90	6.13	6.40	3.95	5.63	7.53
K_2O	1.82	1.32	1.65	2.71	3.66	3.19	3.15	3.72	4.60	3.90	3.62	5.11	6.34	6.11	5.13
P_2O_5	0.99	0.08	0.17	0.44	0.68	0.39	0.27	0.23	0.26	0.12	0.25	0.17	0.02	0.03	0.03
L.O.I	0.89	0.43	0.76	0.57	0.64	0.74	0.48	0.53	0.51	0.87	0.91	0.48	0.53	0.51	0.93
Total	99.11	99.57	99.24	99.43	99.36	99.26	99.33	99.53	99.47	99.52	99.47	99.49	99.13	99.09	99.07
													Trace elements		
Ba	1460	942	867	4421	1759	3468	615	489	533	7356	9151	4939	195	179	4976
Cr	407	396	421	32	29	27	4	7	5	6	5	7	16	5	4
Ga	25.49	31.14	23.39	27.17	19	23	28.72	28.65	33.5	33.18	20.81	23.48	33.59	41.51	41.83
Nb	14.15	21.38	18.65	44.27	64	38.4	85.49	113	134	45.39	17.97	34.46	133.86	142.51	106.97
Ni	27	63	42	12.6	14.3	17.2	3.6	6	11.4	3.2	4.6	5.8	12.2	4.9	2.7
Rb	18.4	27.6	22.9	25.2	33.6	41.5	46.1	63	82	74.8	23.1	35.3	116	104.3	104.2
Sr	901	443	565	721	678	484	391	357	297	136	178	82	109	43	15
V	61	177	214	12	23	18	11	8	15	4	1	3	9	1	3
Y	26.1	48.5	62.7	22	34	41	23.9	56	41	32.4	11.7	16.4	77.3	64.3	27.1
Zr	127.6	141.3	133.8	50.5	74.1	68.4	417.3	564	762	263.7	37.5	121.4	711.2	618.9	383.9
Ta	1.9	2.7	3.2	2.1	3.4	2.8	4.1	6.5	3.7	3.2	0.8	1.5	11.7	6.5	4.7
Zn	137.4	122.3	113.9	95.9	114.3	139.2	154.5	124.7	177.4	123.8	74.4	77.4	237.9	165.4	178.4
U	0.9	1.8	0.65	1	2	3.4	2.2	3.1	2.7	2.3	0.7	0.8	6.2	5.3	2.6
Th	3.1	6.36	3.98	3.5	8.4	12.7	8.4	11.8	13.2	13.8	12.4	11.9	29.1	22	10.9
Rb/Sr	0.02	0.06	0.04	0.03	0.05	0.09	0.12	0.18	0.28	0.55	0.13	0.43	1.06	2.43	6.95
Y/Ho	23.73	28.53	28.5	24.4	27.64	53.94737	26.56	38.62	22.40	43.2	23.4	27.33	29.73	24.73	24.64
U/Th	0.29	0.28	0.16	0.29	0.24	0.27	0.26	0.26	0.20	0.17	0.056	0.07	0.21	0.24	0.23

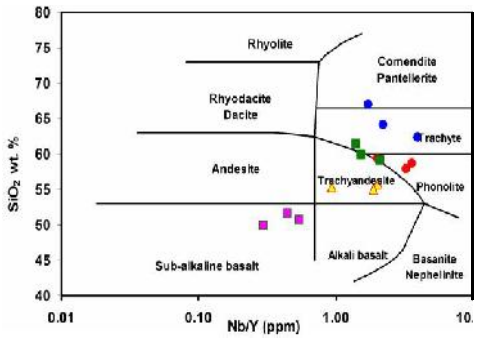

Fig. 13.:Nb/Y versus SiO_2 nomenclature scheme of volcanic rocks after Winchester and Floyd (1977)

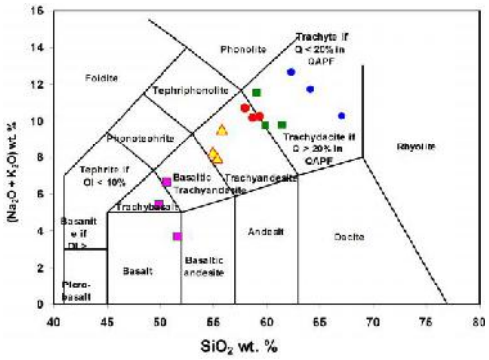

Fig. 14: Total alkali versus SiO_2 classification diagram after Le Bas et al. (1986)

Table 1: Continued

Rock type	Alkali gabbro			Basaltic andesite			Trachyte			Syenite			Trachydacite		
Sample No.	3	11	14	8	13	18	15	19	20	6	10	12	17	25	2
													Rare earth elements (ppm)		
La	36.6	17.3	26.4	34.8	38.4	27.6	52.7	63.4	75.8	69.44	17.5	24.4	117.1	198	76
Ce	78.14	44.2	36.7	71.64	54.31	105.8	103.76	132.7	164.2	86.3	36.81	53.01	237.16	369.17	143.96
Pr	10.9	6.4	8.7	9.6	6.5	4.62	12.7	14.3	17.81	14.6	4.7	6.9	28.2	44.8	16.9
Nd	47.2	38.9	43.2	40.2	32.7	26.4	47.6	51.5	67.12	34.8	19.1	29.1	107.9	169.6	60.9
Sm	9.1	5.8	7.4	7.3	4.8	6.72	7.8	11.74	15.43	7.5	3.5	5.3	20	27.3	9.7
Eu	5.3	3.3	4.1	8.4	5.3	3.64	2.8	2.63	2.48	6.9	8.7	5.2	0.8	1.4	0.9
Gd	7.7	6.5	8.1	7.3	3.5	6.47	6.6	8.3	7.5	7.4	5.9	5.8	17	20.7	6.9
Tb	1.1	0.7	0.98	0.9	1.1	0.87	1	1.53	1.74	0.8	0.5	0.7	2.7	3.2	1.1
Dy	6.4	5.2	4.9	5.1	7.3	4.8	5.1	7.32	9.51	4.8	2.5	3.6	14.1	15	5.4
Ho	1.1	1.7	2.2	0.9	1.23	0.76	0.9	1.45	1.83	0.75	0.5	0.6	2.6	2.6	1.1
Er	2.5	2.87	1.9	2.4	3.67	2.38	2.5	3.57	4.28	2.4	1.2	1.7	7.4	6.9	2.7
Tm	0.3	0.42	0.5	0.3	0.48	0.64	0.4	0.54	0.76	0.3	0.2	0.2	1.1	0.9	0.4
Yb	2	3.12	2.48	2	3.62	4.13	2	4.58	5.98	2.1	1.5	1.7	6.8	6	2.5
Lu	0.3	0.43	0.37	0.3	0.24	0.56	0.3	0.42	0.87	0.3	0.2	0.3	0.9	0.8	0.4
∑REE	209	137	148	191	163	195	246	304	375	238	103	139	564	866	329
Eu/Eu*	1.92	1.63	1.61	3.49	3.93	1.68	1.19	0.81	0.7	2.81	5.81	2.85	0.13	0.18	0.33
$(La/Yb)_N$	12.67	3.84	7.37	12.05	7.34	4.63	18.24	9.58	8.78	22.89	8.08	9.94	11.92	22.85	21.05
$(La/Sm)_N$	2.52	1.87	2.24	2.99	5.01	2.57	4.23	3.38	3.08	5.58	3.13	2.89	3.67	4.55	4.91
$(Eu/Yb)_N$	10.53	3.82	3.99	9.65	4.04	6.9	13.98	7.81	7.4	11.07	6.61	8.4	9.4	16.58	15.51
$TE_{1,3}$	1.01	0.77	0.66	0.96	1.08	1.1	1.03	1.09	1.16	0.98	0.87	0.99	1.04	1.03	1.01

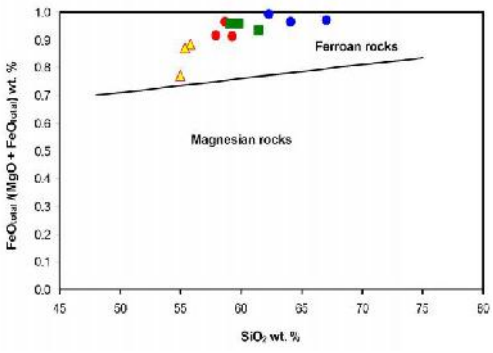

Fig. 15: Classification for feldspathic igneous rocks after Frost and Frost (2008)

the diagram of Frost et al. (2001) on which all studied samples are located in the alkaline field (Fig.16). The rocks of El Gezira alkaline associations are mainly metaluminous, except for few highly evolved rock types. This is indicated by using of A/NK. - A/CNK diagram after Maniar and Piccoli (1989) in which most samples are classified as metaluminous (Fig. 17). Using of Zr versus 10000×Ga/Al binary diagrams (Fig.18) after Whalen et al. (1987), the studied association is located on A-type granite field. On the Rb versus (Y + Nb) diagram (Fig.19) after Pearce et al. 1986, the data plot within plate granite field.

On variation diagrams, relation between SiO_2 wt% and selected major elements (Figs.

Table 1: Continued

Rock type	Alkali gabbro			Basaltic andesite			Trachyte			Syenite			Trachydacite		
Sample No.	3	11	14	8	13	18	15	19	20	6	10	12	17	25	2
A/CNK	0.89	0.96	0.84	0.89	0.85	0.88	0.81	0.85	0.77	0.89	0.89	0.79	0.72	0.90	0.85
A/NK	1.79	3.11	2.11	1.28	1.37	1.41	1.08	1.06	0.99	1.14	1.20	0.94	0.79	0.94	0.87
T. alk	6.64	3.67	5.39	9.56	8.28	7.96	10.18	10.29	10.72	9.80	9.75	11.51	10.29	11.74	12.66
Dif . I	50.06	27.79	38.34	68.48	60.72	59.62	74.71	75.70	75	74.12	73.6	53.83	69.38	86.68	60.29
Fe/Fe+Mg	0.86	0.59	0.67	0.91	0.81	0.90	0.97	0.93	0.93	0.95	0.97	0.97	0.98	0.97	0.99
R1	856.9	2021.7	1282.6	374.8	882.2	916.5	398.01	473.6	322.8	855.8	740.6	202.65	1362.7	682.9	73.3
R2	1229.3	1690.4	1591	882.9	1055.8	952.66	723	653.39	706.9	648.19	757.4	594.05	388.9	401.5	353.4
															CIPW norms
Q	0	0	0	0	0	0	0	0	0	0.83	0	23.45	29.88	2.19	29.66
or	10.88	7.84	9.83	16.12	21.8	19.01	18.76	19.81	27.35	23.18	21.52	30.38	39.5	36.47	30.63
ab	36.81	19.95	24.56	45.42	38.45	40.61	51.26	55.73	42.49	50.11	52.08	0	0	48.02	0
an	20.01	31.26	23.64	9.78	14.19	14.34	2.58	4.29	1.53	6.55	8.65	0	0	1.64	0
ne	2.37	0	3.95	6.94	0.47	0	4.69	0.16	5.16	0	0	0	0	0	0
ns	0	0	0	0	0	0	0	0	0	0	0	12.66	7.82	0	14.95
Di wo	4.31	5.21	8.15	4.12	4.02	3.93	5.97	3.45	5.67	2.8	3.65	4.64	2.6	0.56	0.57
Di en	1.08	2.83	3.9	0.74	1.31	0.84	0.35	0.47	0.78	0.29	0.25	0.31	0.11	0.03	0.01
Di fs	3.48	2.2	4.13	3.71	2.85	3.37	6.33	3.31	5.43	2.81	3.82	4.87	2.8	0.59	0.64
Hy en	0	11.84	0	0	0	1.61	0	0	0	1.14	0.19	0.69	0.46	0.52	0.17
Hy fs	0	9.19	0	0	0	6.49	0	0	0	11.14	3.02	10.68	11.33	9.45	11.8
Ol fo	3.21	4.37	8.7	1.49	3.76	0.81	0.39	1.19	0.98	0	0.27	0	0	0	0
Ol fa	11.41	3.74	10.17	8.24	9.05	3.59	7.82	9.22	7.54	0	4.68	0	0	0	0
il	4.26	1.39	2.6	2.46	2.6	4.56	1.3	1.88	2.5	0.9	1.32	1.43	0.32	0.46	0.81
ap	2.18	0.18	0.37	0.97	1.5	0.86	0.54	0.51	0.57	0.26	0.55	0.37	0.04	0.07	0.07

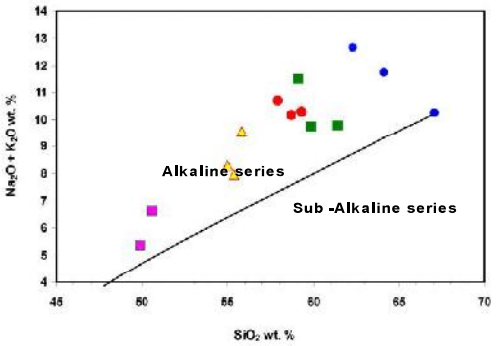

Fig.16: Discrimination diagram between alkaline and sub- alkaline series after Irvine and Baragar (1971)

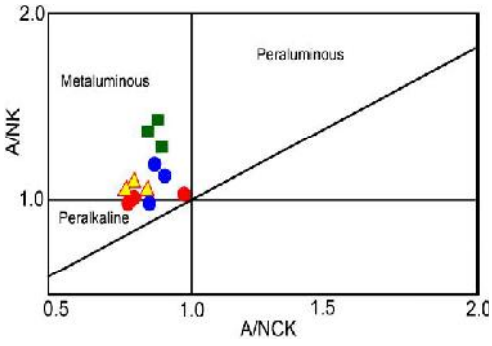

Fig. . 17: A/NK vs. A/CNK binary diagram after Maniar and Piccoli (1989)

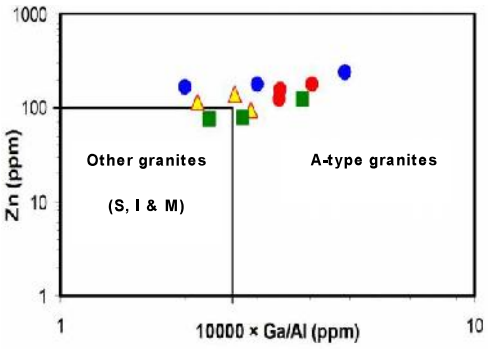

Fig. 18: 10,000 Ga/Al versus Zr plot after Whalen et al. (1987)

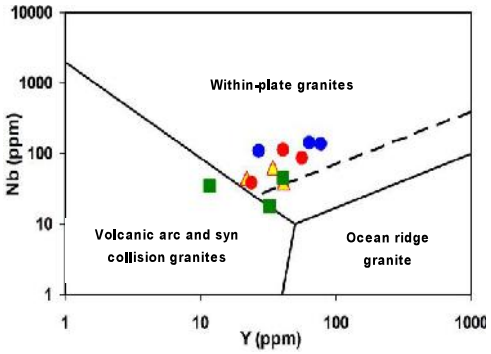

Fig. 19: Y + Nb versus Rb plot after Pearce et al. (1984)

and 13.87 wt% respectively, compared to other rock units. On the other hand, intermediate to acidic association exhibits high orthoclase and albite contents with averages 25.38 and 35.35 wt%, but low anorthite, diopside and olivine with averages 5.29, 7.33, and 4.92 wt% respectively. Normative nepheline is very low for all alkaline association with averages = 1.45 (Table 1).

Regarding trace elements, primitive mantle-Normalized trace-element patterns for these rocks show that they are enriched in U, Th, Rb, Ta, Nb, Zn Ba and Zr, but depleted in P, Ti, Y, Sr, Co, and V (Fig.28). General-

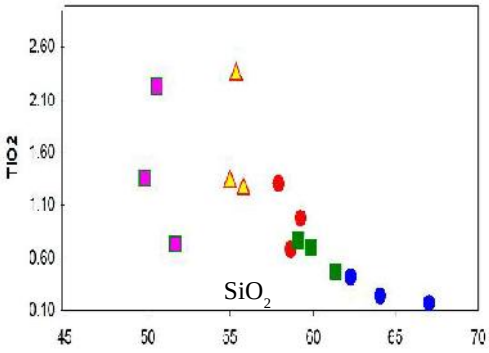

Fig. 20: Variation diagram of SiO_2 wt % and TiO_2 wt%

20 -27) the compositional gap between the basic, intermediate and acidic alkaline association is very small or absent. With increasing SiO_2 the contents of Al_2O_3, FeO_t, MgO, CaO, and TiO_2 show a gradual decrease while the total alkalis possess positive relation . The CaO content shows the highest value in alkali gabbros with average 8.3 wt %, meanwhile other alkaline association contains lesser values with average 3.0 wt %. The agpaitic index (Na+K)/Al) ranging from 0.79 to 3.11 suggests agpaitic composition. The alkali gabbro samples show low normative albite with average 27.11 wt%, and high normative anorthite, diopside and olivine with average 24.97, 11.76

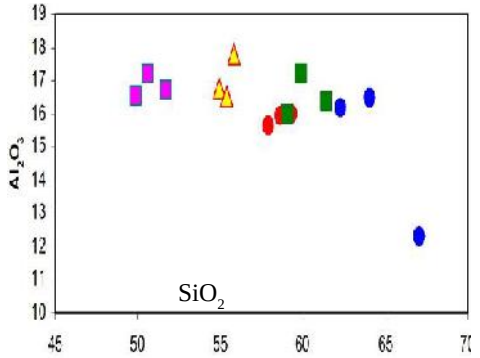

Fig. 21: Variation diagram of SiO_2 wt and Al_2O_3 wt%

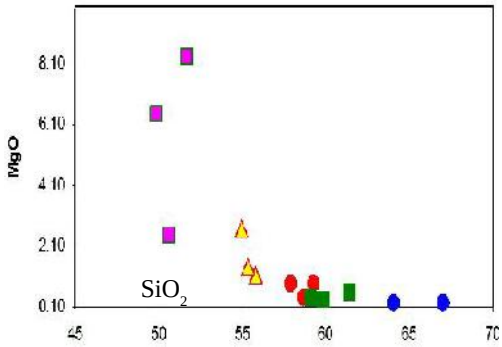

Fig.22: Variation diagram of SiO_2 wt% and MgO wt %

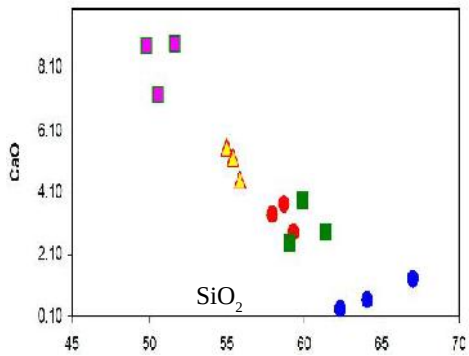

Fig.25: Variation diagram of SiO_2 wt and CaO wt%

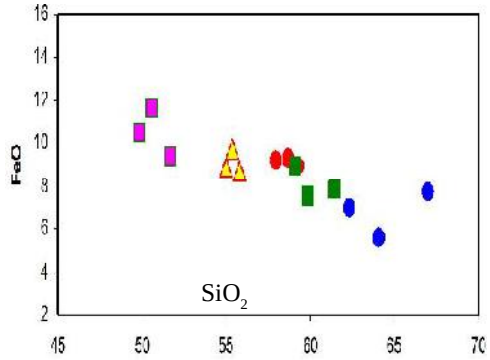

Fig.23: Variation diagram of SiO_2 wt and FeO wt%

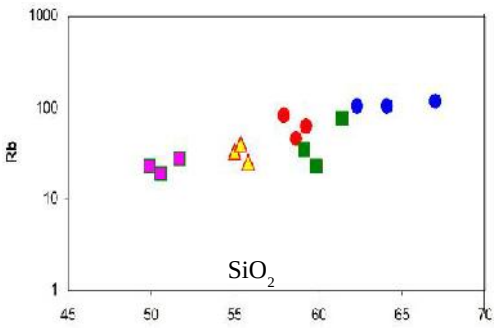

Fig.26: Variation diagram of SiO_2 wt% and Rb (ppm)

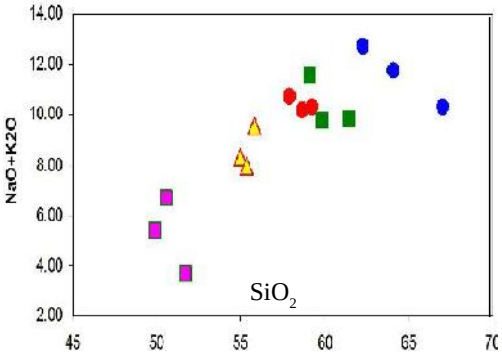

Fig.24: Variation diagram of SiO_2 wt% and total alkalis

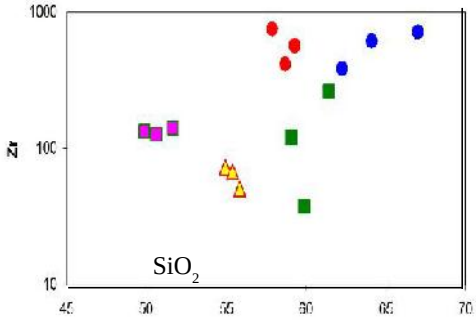

Fig. 27:Variation diagram of SiO_2wt and Zr (ppm)

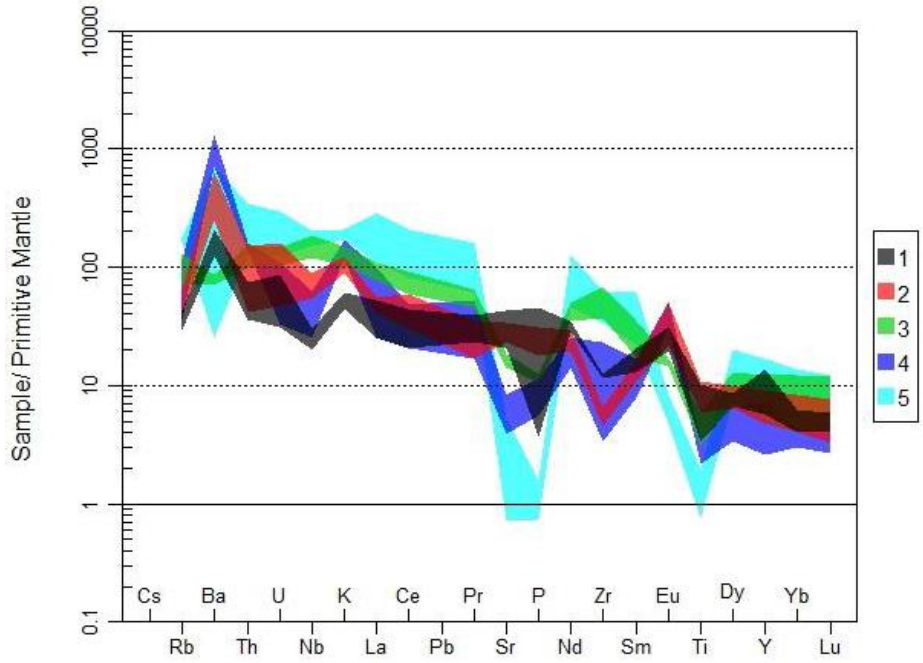

Fig. 28: Primitive mantle (PM) normalized trace elements diagram. (Normalized value are from Sun and McDonough 1989). 1) Alkali-gabbro, 2) basaltic andesite, 3) trachy andesite, 4) syenite, 5) trachy dacite

ly, the compatible trace elements show strong decrease from the alkali gabbros to the more acidic varieties. V, Ni and Cr decrease with increasing the SiO_2 (wt %) for the analysed samples (i.e. Ni decrease from 63 to 3.2 ppm, V decreases from 214 to 1 ppm, Cr decreases from 421 to 4 ppm .

Chondrite normalized trace-element REEs are shown on (Figs. 29-33), based on the chondrite values after Sun and McDonough (1989). El-Gezira alkaline rocks reflect a progressive increase in REEs contents from alkali gabbros (ΣREE = 137–209 ppm), intermediate association (ΣREE = 103– 375 ppm) to trachy-dacite (ΣREE = 328– 866 ppm). REE normalized patterns for essexites are flat and parallel with about 100 time chondrite abundance (Fig. 29). Basaltic andesite shows quite enrichment in

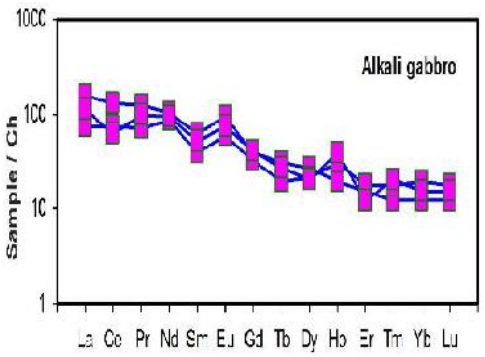

Fig.29: Rare Earth element patterns for essexite

LREE compared to HREE, with (La/Yb)N 4.6 – 12.05, (La/Sm)N = 2.57–5.01, and (Eu/Yb) N = 4.04 – 9.65. The pattern also shows slight positive Eu (Fig.30), with Eu/Eu* ranges 1.68 – 3.93. The same case is noticed in trachy-andesite with slight enrichment in LREE (Fig.31). Syenite and trachy-dacite show higher LREE with $(La/Yb)_N$ = (8.08– 22.89, 11.92 - 22.85), $(La/Sm)_N$ = (2.89 – 5.58, 3.67 – 4.91 and $(Eu/Yb)_N$ = (6.61 – 11.07, 9.4 – 16.58) respectively. Syenite and trachy-dacite REE patterns also show apparent tetrad shape, with positive and negative Eu anomaly with Eu/Eu* = 2.81–5.81 and 0.13–0.33, respectively (Figs.32,33). Based on the calculation mechanism of tetrad effect (TE) after Iber (1999), the calculated ($TE_{1,3}$) for El-Gezira alkaline rock has range (0.66 - 1.16) with average = 0.98.

DISCUSSION

Temperature of Magmatic Crystallization

Most rock units of El-Gezira alkaline ring complex are metaluminous and display geochemical signatures of A-type magmatic nature (Eby, 1990). Temperature of El-Gezira magma is calculated here using apatite (A_P) and monazite (M_Z) saturation thermometers after (Harrison and Watson, 1984) and

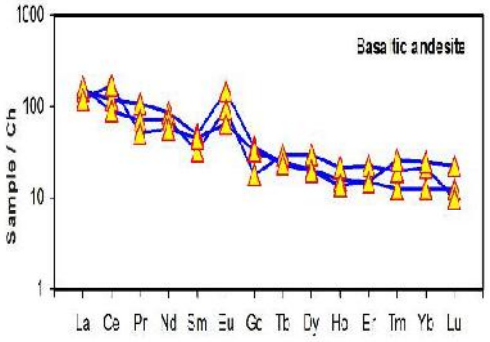

Fig.30: Rare Earth element patterns for basaltic andesite

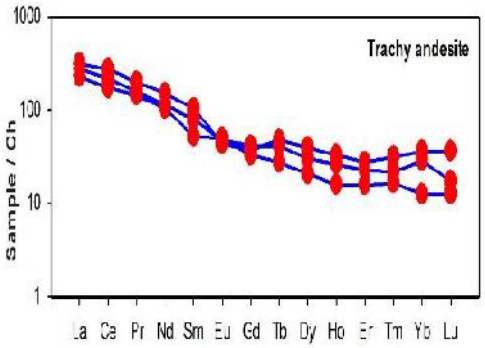

Fig.31 : are Earth element patterns for trachy andesite

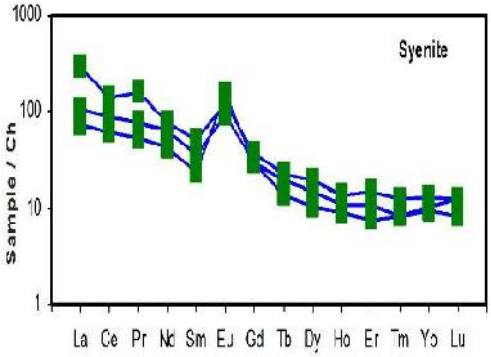

Fig.32 :.Rare Earth element patterns for syenite

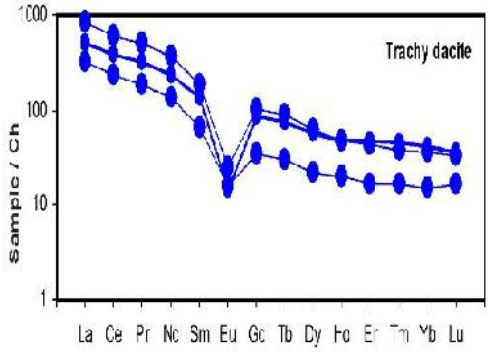

Fig.33: Rare Earth element patterns for trachy dacite

(Montel, 1993), respectively. The calculated (T_{Ap}) temperature are 651– 963° C for essexite gabbro , 889 – 966 °C for basaltic andesite, 872– 889 °C for trachy-andesite, 827–892 °C for syenite and 701–740 °C fore trachy-dacite. Moreover, monazite saturation temperatures (T_{Mz}) are significantly low and range from 595 to 652°C for essexite gabbro, 655 – 682°C for basaltic andesite, 682–725 °C for trachy-andesite, 657–736°C for syenite and 769 –901 °C for trachy-dacite.

Crustal Assimilation and Magmatic Recycling

The studied ring complex is characterized by the existence of intelligible display of both plutonic and volcanic alkaline rock verities which is relatively different from most alkaline associations from the Egyptian Shield. All rocks types have A/CNK values < 1 with range (0.77–0.96). Most variation diagrams show similarity in their trends and relationships with silica with very small or no gabs. It may be assumed that the highly evolved intermediate and acidic association can be formed as fractionation product from the least evolved mafic suite. The mafic lithology has flat REE patterns with no Eu anomalies suggesting that these materials may represent the parental basaltic mantle melt from which the rest of El Gezira ring complex may be evolved.

Possible assimilation and mixing between magmas of different composition are widely recognized. The existence of mafic enclaves (Bacon and Metz, 1984; Bacon, 1986; Koyaguchi, 1986) can give a clue for the incomplete magma mixing. Reversely zoned crystals and the elevated contents of compatible elements may indicate more complete mixing (Luhr and Carmichael, 1980; Shimizu and Roex, 1986; Novak and Bacon, 1986). El-Gezira alkaline association has several petrographic and chemical data that can support the hypothesis of magma recharge or mixing as follow: (a) most plagioclase and pyroxene phenocrysts exhibit complex zoning structures, (b) complete or partial resorption of phenocrysts, (c) existence of embayed crystals, the develop of epitaxitic pyroxene crystal growth around xenocryst of quartz. All the above can confirm that the phenocrysts were not in thermal and chemical equilibrium with the host magma. Changes in CaO, Na_2O and K_2O, contents in the El-Gezira rocks are interpret through fractionation of feldspars. The wide differences in alkalinity ratios may be ascribed to contamination from high-K magma at the source region and minor crustal mixing at final intrusion/or emplacement environments. The relatively high Na_2O contents ~7 wt % in some andesite and dacite rocks may ascribed to the interaction between of seawater and the alkaline lithologies during the ring complex emplacement. Generally, the alkaline association of El-Gezira shows linear patterns with distinct scatter for compatible major oxides and trace elements in the variation diagrams (Fig. 20-29). The linear behavior and the sprinkle of some data may demonstrate magma mixing and/or assimilation by the two end members (Reid et al., 1983; Kistler et al., 1986; Frost and Mahood, 1987). The scatter in some data may be resulted from different rates of contamination, recycling and assimilation from different magma sources in addition to fractionation processes. The distinguished Eu anomalies recorded in the REE pattern (Figs. 29-33), (the basaltic andesite, syenite samples) and the negative Eu anomalies observed in more evolved rocks (tracy- dacite), can be account for crystal accumulation mechanisms. The petrographic criteria of cumulate textures, the scatter of most trace element data, and the positive Eu anomalies all are indicative of plagioclase accumulation during crystallization (Barnes et al., 2016). The trachy-dacite shows unambitious Sr/Y values and the most distinguished negative Eu anomaly compare to other samples. This suggests a melt from a shallow crustal level that retained Eu in plagioclase at the source. In contrast alkali gabbro and basaltic andesite samples have high Sr/Y ratio and low LREEs compared to other rocks units, suggesting magma derived from a much deeper source (Gromet and Silver, 1987). The alkaline rocks that are formed in subduction setting or derived from magmas which were

modified by subduction events, usually have a pronounced negative Nb (i.e. Rogers et al., 1985; Nelson and McCulloch, 1989). Meanwhile alkaline suites from rift zones or oceanic island settings show no or slightly positive Nb (MacDonough, et al., 1985; Menzies, 1987). According to MacDonough, et al. (1985); Fitton (1987), the intraplate hot spot alkaline magmas are explained as being related to plume activities. Therefore, the source magma of El-Gezira ring complex may be derived from Nb enriched or at least under-plated mantle source within the continental crust.

Tetrad Effect and Possible Economic Importance

The term "tetrad effect" refers to the sub-division of the fifteen members of the REE series into four groups with "breaks" at Gd, between Nd and Pm, and between Ho and Er, corresponding to the 1/2, 1/4, and 3/4-filled 4f subshell, respectively. The calculated $TE_{1,3}$ values of the tetrad effect range from 1.00 for a REE pattern without tetrad effect, toward higher values ($TE_{1,3} > 1$) for REE patterns with tetrad effects (Zhao et al., 1993; Lee et al., 1994, Bau, 1996; Irber, 1999). The REE patterns of El-Gezira alkaline association are characterized by existence of tetrad effects which can be observed from the REE patterns (Figs. 30,32,33) and also from the calculations using formula after Irber (1999), (Table 1). Monecke et al. (2002) supposed that the tetrad pattern is mostly visible in highly evolved leucogranites, pegmatites and mineralized granites. It is either a feature of the magmatic-fluid system before magmatic crystallization or it may be inherited from external fluid during or after the emplacement of the magma. The tetrad effect in El-Gezira may reveal the highly evolved nature and the effect of hydrothermal activities during the evolution of these rocks. Such fluids may be responsible for enrichment of many rare metals in association with the studied ring complex. El-Gezira alkaline association has relatively high contents of Ta, and Nb with an average of 4 and 68 ppm respectively. Similarly, high values are noticed from previous studies on El-Gezira association. Mohamed (1998) recorded Nb value up to 280 ppm in the highly evolved trachy-dacite from El-Gezira. Figure (34) shows comparative relation between average contents of Nb and Ta in El- Gezira alkaline rocks and in famous classical Ta-Nb bearing granites/pegmatites. It is clear that the studied association has high Nb/Ta ratios that generally progressively increase from the less evolved to the highly fractionated units in El-Gezira area. The studied association shows quiet concordance with most Ta, Nb bearing deposits in the Nubian Shield. El-Gezira association shows relatively lower concentration of Ta but still has higher values compared to Igla famous mine (Fig.34). Moreover, Nb shows higher values compared with Homr Akarem & Homret Mukbid, Nuweibi, Muelha, and Igla from Egyptian Eastern Desert (Fig.34). Consequently, El-Gezira alkaline association may present a new concession for Nb/Ta rare metal prospecting, however more information is still needed to elucidate the ore reserve and zones of enrichment.

GEODYNAMIC IMPLICATIONS

On a global scale, most of the continental provinces of ring complexes are located in cratons,i.e. tectonically stable regions of the crust (Sorensen, 1974). Moreover, the association of most of these alkaline provinces with zones of rift is well established **(** Maurin and Guiraud, 1993**)**. These zones of rift are the fractured crests of crustal arches. The cause of swelling and up-doming of the crust is thought to be an intraplate mantle hot spot (Wright, 1973) where parts of the plate overlying positive thermal anomalies are heated by the rising convection columns in the mantle (Briden and Gass, 1974). Emplacement of the post-orogenic or anorogenic complexes in NE Africa took place during an extended period of time spanning almost the entire Paleozoic and Mesozoic eras (Vail, 1990). At these times, Gondwana land witness a long period of fragmentation as result of the extension between South America and Africa. The tectonic interplay between oceanic and conti-

nental terrains causes re-initiation of the deep-seated fractures and enhance breakup of the African terrains. The north extension of the ANS was traversed by a major Late Precambrian 630 and 530 Ma transform movement named the Najd Fault System (NFS) (Stern, 1985). This corridor outlines zone around 400-km across with NW–SE trending crustal extension. In Egypt, the NFS is manifested by a set of NW-trends i.e. Duwi fault zone, steeply dipping ductile shear zones i.e. Wadi Kharite-Wadi Hodein shear zone, and folds, in addition to widespread granite magmatism (Fritz et al., 1996, 2002, 2013; Johnson et al., 2011). Detailed regional mapping coupled with geophysical investigations for deep seated fractures in the NS revealed their wide association with alkaline intrusions (Fig. 1), (Morsey and Mohamed, 1992; AbdelRahman, 2006). Fowler and Hamimi (2020) explained different views on the regional scale and zone of influence by the Najd Fault System in the (ANS). They assumed that transpression regime related to NFS plays a greater role in casting nearly all areas of the CED and large parts of the SED (from the Duwi to the Wadi Kharit-Wadi Hodein shear zones) within the Najd Fault Zone (Fig. 1). Based on that, the Egyptian Neo-proterozoic cover is supposed to coupled major rift systems that believed to be responsible for deep seated fragmentations and related magmatism:

(a) NE–SW transform faults along red sea rifting, and (b) spectrum of strike-slip faults trending NW–SE along famous Allaqi-Heinai suture zone (Fig. 1). Hence, the Egyptian ring complexes can be related to swells or arches in the crust essentially distributed at random, but with some alignment along lines of weakness which probably existed since Precambrian times and suffered frequent rejuvenation. Structurally, the emplacement of El-Gezira alkaline ring complex in the Southeastern Desert allocate along the intersection of two old regional fracture systems: The transform faults and the NW deep fracture zones. Tectonic evaluation model showing the simplified evolutionary history for El-Gezira caldera complex is considered in this study (Fig.35). Three evolutionary stages are suggested to explain the geodynamic setting and eruptive cycles at El-Gezira area as follows:

a) Pre caldera phase is the early stage that

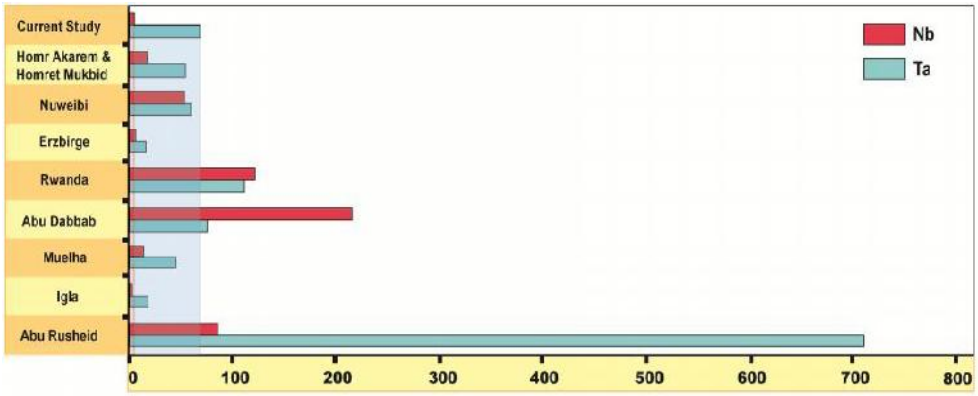

Fig. 34: Comparison between average contents of Ta & Nb in El-Gezira alkaline rocks and reference data from famous rare metal bearing suites. A) Present study, B) Homr Akarem and Homret Mukbid after (Ali et al. 2012), C) Nuweibi after (Emam et al. 2018), D) Erzbirge from Palchen et al. 1987, E) Rwanda after Lehmann et at. 2014), F) Abu Dabbab after Heikal et al. 2019, G) Muelha after Abu El- Rus et al. 2017, H) Igla after Hassanen et al. 1996, I) Abu Rusheid after Ali et al. 2011.

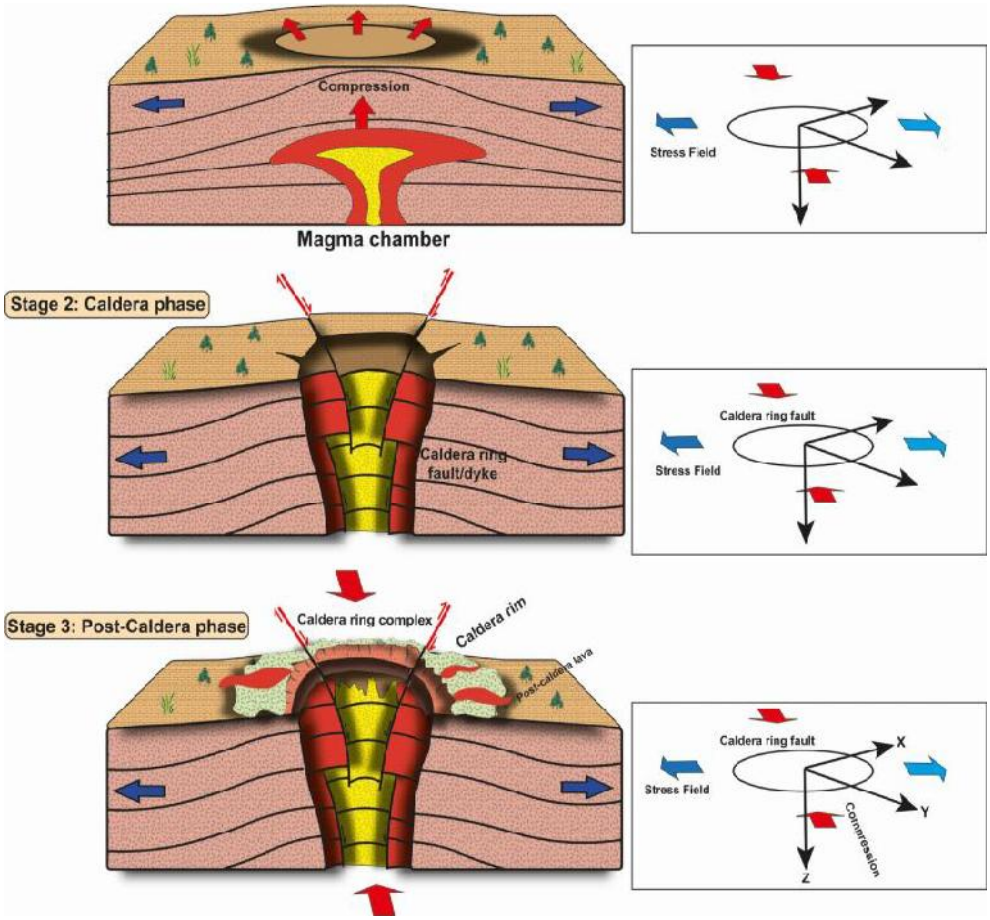

Fig. 35 : Sketch diagram explains the evolution and emplacement stages of El –Gezira ring complex

assumed to be initiated by deeply intrusion of cone like sheets derived from an underlying magma chamber. This early emplaced magma has mantle signature which should be basic suites in El-Gezira area (essexite, basaltic andesite). Such magmas are believed to become over pressured and start to dome or expand upward. Such expansion may preserve the suitable circumstances desired to break up the overlying units and facilitate intrusion of the caldera cone structure.

b) Caldera phase occurs as a piston style caldera collapse. At this stage the mafic melts may supposed to fractional crystallization lead to formation of the more evolved and the oversaturated syenitic magmas (syenite and trachyte suites). The wide initiation of the deep-seated fractures and the deflation of the chamber during intrusion of the cone sheets may lead to the partial collapse of the enclosed area into the underlying magma chamber resulting in crustal contamination and recharge

of the original melt.

C) Post caldera phase represents the final stage of caldera formation and is generated by extreme extension. At this stage and extensive fractionation and crustal assimilation continued lead to the formation of the highly evolved suites (trachy-dacite). The relatively high temperature of magmas, decrease in density due to assimilation, and the action of liquids could promote migration of this juvenile magma to shallow levels in the crust.

CONCLUSIONS

1-El-Gezira alkaline association is characterized by the existence of plutonic and volcanic alkaline rocks namely: essexite gabbro, basaltic andesite, trachyte, trachy-andesite, trachy-dacite, monzosyenite, carbonatized syenite, and aegirine bearing syenite.

2-El-Gezira rocks are alkaline with metaluminous nature. They have low values of CaO, MgO, Sr and high concentrations of alkalis, Rb, Nb, Y, and REE.

3-El-Gezira alkaline association is classified as A-type granites that formed in anorogenic setting.

4-The parental magma of El-Gezira may be produced from an Nb-enriched mantle source. This magma can be subjected to minor crustal contamination through their fractional crystallization.

5-Development of El-Gezira alkaline association is explained as caldera type volcano formed during an-orogenic times through reactivation of deep-seated fractures.

6-The relatively high contents of Nb in the studied units should be considered in the future prospecting for rare metals. However further studies still needed to infer the mineralized zones and ore reserve.

Acknowledgements

The authors highly thanks the Geology Department, Faculty of Science, Aswan University, for allowing the field and laboratory facilities. Special thanks to Prof. Ezzat Abdel-Rahman, professor of mineralogy, Faculty of Science, Aswan University, for his participating in the field work.

Conflict of interests

The authors declare no conflict of interest.

REFERENCES

Abdel-Rahman, A. M., 2006. Petrogenesis of anorogenic peralkaline granitic complexes from eastern Egypt. Mineralogical Magazine, 70(1), 27-50.

Abu El-Rus, MA.; Mohamed MA.; Lindh A., 2017. Mueilha rare metals granite, Eastern Desert of Egypt: An example of a magmatic-hydrothermal system in the Arabian-Nubian Shield. Lithos, 294, 362-382.

Ali M.A.; Lentz D.R.; Hall D.C., 2011. Mineralogy and geochemistry of Nb-, Ta-, Sn-, U-, Th-, and Zr-bearing granitic rocks from Abu Rusheid shear zones, south Eastern Desert, Egypt. Chinese J. Geoch., 30(2), 226-247.

Ali K.A.; Moghazi A.; Maurice A.E.; Omar S.A.; Wang Q.; Wilde S.A.; Moussa E.M.; Manton W.I.; Stern R.G., 2012. Composition, age, and origin of the ~620Ma Humr Akarim and Humrat Mukbid A-type granites: no evidence for pre-Neoproterozoic basement in the Eastern Desert, Egypt. Int. J. Earth Sci. (Geol Rundsch), 101,1705–1722.

Bacon, C. R.,1986. Magmatic inclusions in silicic and intermediate volcanic rocks. J. Geophysical Res.: Solid Earth, 91(B6), 6091-6112.

Bacon, C. R.; and Metz, J.,1984. Magmatic inclusions in rhyolites, contaminated basalts, and compositional zonation beneath the Coso volcanic field, California. Contributions to Mineralogy and Petrology, 85(4), 346-365.

Barnes, C. G.; Coint, N., and Yoshinobu, A.,2016. Crystal accumulation in a tilted arc batholith. Amer. Mineral., 101(8), 1719 – 1734.

Bau, M.,1996. Controls on the fractionation of isovalent trace elements in magmatic and aqueous systems: evidence from Y/Ho, Zr/Hf, and lanthanide tetrad effect. Contributions to Mineralogy and Petrology, 123(3), 323-333.

BAS, M. L.; Maitre, R. L.; Streckeisen, A.; Zanettin, B., IUGS Subcommission on the Systematics of Igneous Rocks,1986. A chemical classification of volcanic rocks based on the total alkali-silica diagram. J. petrology, 27(3), 745-750.

Black, R.; Lameyre, J.; and Bonin, B.,1985. The structural setting of alkaline complexes. J. Afri. Earth Sciences , 3(1-2), 5-16.

Briden J.C., and Gass I.G.,1974. Plate movement and continental magmatism. Nature, Land., 248, 650 -653.

Eby, G. N.,1990. The A-type granitoids. In: a review of their occurrence and chemical characteristics and speculations on their petrogenesis. Lithos, 26(1-2), 115-134.

El-Gaby, S.; List, F. K., and Tehrani, R.,1988. Geology, evolution and metallogenesis of the Pan-African belt in Egypt. In: The Pan-African belt of Northeast Africa and adjacent areas; tectonic evolution and economic aspects of a late proterozoic Oregon, 17-68.

El-Ramly, M. F.; and Hussein, A. A.,1982. The alkaline ring complexes of Egypt. Geol. Surv. Egypt, 63.

El Ramly, M. F., and Hussein, A. A. A., 1985. The ring complexes of the Eastern Desert of Egypt. J. Afri. Earth Sciences, 3(1-2), 77-82.

El Ramly, M. F.; Budanov, V. I.; Hussein, A. A., and Dereniuk, N. E., 1970 . Ring complexes in the south Eastern Desert of Egypt. In: Studies on Some Mineral Deposits of Egypt. Geol. Surv. Egypt, 181-194.

El Ramly M.F.; Budanov V.I., and Hussein A.A.A., 1971. The alkaline rocks of south eastern Egypt. Geol. Surv. Egypt, 53, 111 p.

Emam A.; Zoheir B.; Radwan A.M.; Lehmann B.; Zhang R.; Fawzy S., and Nolte N., 2018. Petrogenesis and evolution of the Nuweibi rare-metal granite, Central Eastern Desert, Egypt. Arab. J. Geosci., 11 (23), 736.

Fitton J.G., 1987. “The Cameron Line, West Africa: A Comparison between Oceanic and Continental Alkaline Volcanism.” In : Alkaline Igneous Rocks (Fitton, J. G., and Upton, B. G. Eds). J. Geol. Soc. Spec., 30, 273-91.

Fowler A.R., and Hamimi Z., 2020. Structural and tectonic framework of Neoproterozoic basement of Egypt: from gneiss domes to transpression belts. In: The geology of Egypt. Springer, Cham. , 81-129.

Fritz H.; Wallbrecher E.; Khudeir A.A.; Abu El Ela F., and Dallmeyer D.R. ,1996. Formation of Neoproterozoic metamorphic complex during oblique convergence (Eastern Desert, Egypt). J Afri. Earth Sci., 23,311–329.

Fritz H.; Dallmeyer D.R.; Wallbrecher E.; Loizenbauer J.; Hoinkes G.; Neumayr P., and Khudeir A.A., 2002. Neoproterozoic tectonothermal evolution of the Central Eastern Desert, Egypt: a slow velocity tectonic process of core complex exhumation. J. Afri. Earth Sci., 34,137–155

Fritz, H.; Abdelsalam, M.; Ali, K. A.; Bingen, B.; Collins, A. S.; Fowler, A. R., and Viola, G., 2013. Orogen styles in the East African Orogen. In: a review of the Neoproterozoic to Cambrian tectonic evolution. J. Afri. Earth Sci., 86, 65-106.

Frost, B.R., and Frost, C.D., 2008. A geochemical classification for feldspathic igneous rocks. J. Petrol., 49(11), 1955-1969.

Frost, B.R.; Barnes, C.G.; Collins, W.J.; Arculus, R.J.; Ellis D.J., and Frost C.D., 2001. A geochemical classification for granitic rocks. J. petrol., 42(11), 2033-2048.

Frost, T.P., and Mahood, G.A., 1987. Field, chemical, and physical constraints on mafic-felsic magma interaction in the Lamarck Granodiorite, Sierra Nevada, California. Geol. Soci. Ame. Bull., 99(2), 272-291.

Garson, M.S., and Krs, M., 1976. Geophysical and geological evidence of the relationship of Red Sea transverse tectonics to ancient features. Bull. Geol. Soc. Am. , 87, 169–181.

Gromet, P., and Silver, L. T., 1987. REE variations across the Peninsular Ranges batholiths . In: Implications for batholithic petrogenesis and crustal growth in magmatic arcs. J. Petrol., 28(1), 75-125.

Harrison, T.M., and Watson, E.B., 1984. The behavior of apatite during crustal anatexis—equilibrium and kinetic considerations. Geochim Cosmochim Acta, 48, 1467–1477.

Hashad, A.H., and El Reedy, M.W.M., 1979. Geochronology of the anorogenic alkalic rocks south Eastern Desert, Egypt. Ann. Geol. Surv. Egypt, IX, 81–101.

Hassanen, M.A.; El-Nisr, S.A. , and Mohamed, F.H.,1996. Geocheinistry and petrogenesis of Pan- African I-type granitoids at Gabal Igla Ahmar, Eastern Desert, Egypt. J. Afri. Earth Sci., 22 (1), 29-42.

Heikal, M.T.S.; Khedr, M.Z.; Abd El Monsef, M., and Gomaa, S.R., 2019. Petrogenesis and geodynamic evolution of neoproterozoic Abu Dabbab albite granite, central Eastern Desert of Egypt. In: petrological and geochemical constraints. J. Afri. Earth Sci., 158, 103518.

Iber, W., 1999. The lanthanide tetrad effect and its correlation with K/Rb, Eu/Eu*, Sr/Eu, Y/Ho, and Zr/Hf of evolving peraluminous granite suites. Geochim Cosmochim Acta, 63,489–508.

Johnson, P. R.; Andresen, A.; Collins, A. S.; Fowler, A. R.; Fritz, H., Ghebreab, W., and Stern, R. J., 2011. Late Cryogenian–Ediacaran history of the Arabian–Nubian Shield: a review of depositional, plutonic, structural, and tectonic events in the closing stages of the northern East African Orogen. J. Afri. Earth Sci., 61(3), 167-232.

Liegeois, J.P.; Navez, J.; Hertogen, J., and Black, R., 1998. Contrasting origin of post-collisional high- K calc-alkaline and shoshonitic versus alkaline and peralkaline granitoids. The use of sliding normalization. Lithos, 45(1-4), 1-28.

Kistler, R. W.; Chappell, B. W.; Peck, D. L., and Bateman, P. C., 1986. Isotopic variation in the Tuolumne intrusive suite, central Sierra Nevada, California. Contributions to Mineralogy and Petrology, 94(2), 205-220.

Koyaguchi, T., and Blake, S., 1991. Origin of mafic enclaves; constraints on the magma mixing model from fluid dynamic experiments. Enclaves and granite petrology. Developments in Petrology, 13, 415–429.

Lee, S. G.; Masuda, A., and Kim, H. S., 1994. An early Proterozoic leuco-granitic gneiss with the REE tetrad phenomenon. Chem. Geol., 114(1-2), 59-67.

Lehmann, B.; Halder, S.; Munana, J.R.; Ngizimana, J., and Biryabarema, M., 2014. The geochemical signature of rare-metal pegmatites in Central Africa: magmatic rocks in the Gatumba tin–tantalummining district, Rwanda. J Geochem. Explor., 144, 528–538.

Luhr, J. F., and Carmichael, I. S., 1980. The colima volcanic complex, Mexico. In: Contributions to Mineralogy and Petrology, 71(4), 343-372.

MacDonough, W.F.; McCulloch, M.T., and Sun, S.S., 1985. Isotope and Geochemical Systematics in Tertiary-Recent Basalts from South-Eastern Australia and Implications from the Evolution of the Sub-continental Lithosphere. Geochem. Cosmo. Acta , 49, 2051-67.

Maurin, J.C., and Guiraud, R., 1993. Basement control in the development of the Early Cretaceous West and Central African rift system. Tectonophysics, 228(1-2), 81-95.

Menzies, M., 1987. “Alkaline Rocks and Their Inclusions: A Window on the Earth’s Interior. In :Alkaline Igneous Rocks (Fitton, J. G., and Upton, B. G. J., Eds.). Geol. Soc. Spec., 30, 15-27.

Mohamed, F.H., 1998. Geochemistry and petrogenesis of El Gezira ring complex, Egypt. In: a monzosyenite cumulate derived from fractional crystallization of trachyandesitic magma. J. volcanology and geothermal

research, 84(1-2), 103-123.

Monecke, T.; Kempe, U.; Monecke, J.; Sala, M., and Wolf, D., 2002. Tetrad effect in rare earth element distribution patterns: a method of quantification with application to rock and mineral samples from granite-related rare metal deposits. Geochim. Cosmochim. Acta, 66, 1185–1196.

Montel, J.M., 1993. A model for monazite/melt equilibrium and application to the generation of granitic magmas. Chem. Geol., 110(1-3), 127-146.

Morsey, M.A., and Mohamed, F.H., 1992. Geochemical characteristics and petrogenetic aspects of Muelha tin-specialized granite, Eastern Desert, Egypt. Bull Fac. Sci., Alex. Univ., 32(A), 502–515

Nelson, D.R., and McCulloch, M.T., 1989. Enriched Mantle Components and Mantle Recycling of Sediments. In: Kimberlites and Related Rocks, 1, Their Composition, Occurrence, Origin and Emplacement (Ross, J., Ed.). Geol. Soc. Aust., 14, 560-70.

Novak, S.W., and Bacon, C.R., 1986. Pliocene volcanic rocks of the Coso Range, Inyo county, California.

Oftedahl, C., 1978. Cauldrons of the Permian Oslo rift. J. Volcanology and Geothermal Research, 3, 343–371.

Pälchen, W.; Rank, G.; Lang, H., and Tischendorf, G., 1987. Regionale Clarkewerte Moglichkeiten und Grenzen ihrer Anwendung am Beispel des Erzgebirges (DDR). Chem. Erde, 47,1–17.

Pearce, J.A.; Harris, N.W., and Tindle, A.G., 1984. Trace element discrimination diagrams for the tectonic interpretation of granitic rocks. J. Petrol., 25, 956–983.

Reid, Jr JB.; Evans, O.C., and Fates, D.G., 1983. Magma mixing in granitic rocks of the central Sierra Nevada, California. Earth and Planetary Sci. Letters, 66, 243-261.

Rogers, N.W.; Hawkesworth, C.J.; Parker, R.J., and Marsh, J.S., 1985. The geochemistry of potassic lavas from Vulsini, central Italy and implications for mantle enrichment processes beneath the Roman region. Contri. Mineral. and Petrol., 90(2-3), 244-257.

Richey, J.E., 1948. British regional geology: Scotland. In: The Tertiary volcanic districts (second edition, revised): De-partment of Scientific and Industrial Research, Geologi-cal Survey and Museum, Great Britain, 49–97.

Schandelmeier, H., and Pudlo, D., 1990. The Central-African Fault Zone in Sudan—a possible continental transform fault. Berliner Geowiss. Abh., 120 A, 31–44.

Shimizu, N., and Le Roex, A.P., 1986. The chemical zoning of augite phenocrysts in alkaline basalts from Gough Island, South Atlantic. J. Volcanology and Geothermal Research, 29(1-4), 159-188.

Smith, R.L., and Bailey, R.A., 1968. Resurgent cauldrons: Geological Society of America Memoir, 116, 613–662.

Sorensen, H., 1974. The Alkaline Rocks. John Wiley, London.

Stern, R.J., 1985. The Najd Fault System, Saudi Arabia and Egypt. In: a Late Precambrian rift related transform system? ,Tectonics, 4, 497–511

Sun, S.S., and McDonough, W.F., 1989. Chemical and isotopic systematics of oceanic basalts: implications for mantle composition and processes. In: Magmatism in the ocean basins (Saunders, A.D., and Norry, M.J., Eds). Geol. Soc. Lond. Spec. Publ., 42, 313–345.

Turner, D.C., 1963. Ring-structures in the Sara-Fier younger granite complex, northern Nigeria. Quarterly J. Geol. Soci., 119(1-4), 345-366.

Vail, J.R., 1985. Pan-African (late Precambrian) tectonic terrains and the reconstruction of the Arabian-Nubian Shield. Geol., 13(12), 839-842.

Vail, J. R., 1989. Ring complexes and related rocks

in Africa. J. Afri. Earth Sci. (and the Middle East), 8(1), 19-40.

Vail, J.R., 1990. Geochronology of the Sudan. Overseas Geology and Mineral Resources, 66, 58pp

Whalen, J.B.; Currie, K.L., and Chappell, B.W., 1987. A-type granites: geochemical characteristics, discrimination and petrogenesis. Contri. Mineral. Petrol., 95, 407–419.

Williams, H., 1941. Calderas and their origin. Bull. Geol. Sci. Dep., 25, 239-346.

Winchester, J.A., and Floyd, P.A., 1977. Geochemical discrimination of different magma series and their differentiation products using immobile elements. Chem. Geol., 20, 325-343.

Wright, J. B. 1973. Continental drift, magmatic provinces and mantle plumes. Nature, Lond., 244, 565-567.

Zhao, Z.H.; Masuda, A., and Shabani, M.B., 1993. REE tetrad effects in rare-metal granites. Chin. J. Geochem., 12, 206–219.

بترولوجية وتكتونية المعقدات الحلقية فى جنوب الصحراء الشرقية: دراسة حالة التجمعات القلوية فى معقد الجزيرة

عبدالهادى رضوان ، اشرف امام ، جيهان بكر الشايب و محمد حسن يونس

يمثل معقد الجزيرة احد الظواهر الهامة للتجمعات القلوية فى جنوب الصحراء الشرقية حيث يظهر معقد الجزيرة على شكل حلقى واضح ويتكون من عدد كبير من الصخور المختلفة التركيب. يتكون تداخل الجزيرة من عدة حلقات متحدة المركز ومفصولة باشكال قوسية من الجابرو القلوى والمقذوفات البركانية وبعض الصخور الهجيينية. تتكون الحلقة الخارجية للجزيرة من صخور البركانيات المتحولة وتدفقات البازلت الانديزيتى. الحلقات الداخلية مكونة من صخورالمونزوسيانيت والسيانيت الحامل للبيروكسين والكربونات والتراكيت والتراكى انديزيت والتراكى داسيت. البيروكسين المعينى هو النوع السائد فى غالبية صخور المنطقة. بينما الامفيبول والالفين يتواجدان فقط فى الصخور القاعدية للمنطقة. يحتوى معقد الجزيرة على عدد كبير من الشروخ والفوالق اغلبها يتجة فى ناحية الشمال الغربى والشرقى للمنطقة. واظهرت التحاليل الكيميائية ان غالبية صخور المنطقة هى صخور ميتالومينية وتحتوى بصورة عامة على تركيزات منخفضة من الكالسيوم والماغنسيوم والسترانشيوم. بينما يحتوى على نسب عالية من الصوديوم والبوتاسيوم و الربيديوم والنيبيوم والعناصر الارضية النادرة. تعطى صخور معقد الجزيرة انماط مختلفة لسلوك العناصر الارضية النادرة حيث تعطى شكل مسطح فى الجابرو القلوى بينما تعطى صخور السيانيت والتراكى انديزايت والتراكى داسيت انماط مجزئة. ويعتبر معقد الجزيرة تابع للصخور البعدية التى تكونت على سطح القارة حيث يعتقد ان الصهارة الاولى قد تكونت فى منطقة الوشاح العلوى ثم انتقلت الى مناطق صهيرية فى منطقة القشرة اثناء عمليات التباعد القارى. وقد تاثرت هذة الماجما بواسطة عمليات التفارق الصهيرى مما ادى الى تكوين ماجما جديدة اقل قاعدية. ومع استمرار عمليات التفارق الصهيرى وزيادة المحاليل الحارة واحتمالية حدوث تماثل لصخور ارضية اقدم ادى الى تكون هذا التسلسل المجماتى القلوى مالئا للكسور والشروخ التى تكونت اثناء الحركات المابعدية.